CaF₂/ZnS Multilayered Films on Top-Emission Organic Light-Emitting Diode for Improving Color Purity and Moderation of Dark-Spot Formation

Naoya Satoh, Tsubasa Tanno, Takuya Kitabayashi, Takayuki Kiba,* Midori Kawamura, and Yoshio Abe

ACCESS | Metrics & More | Article Recommendations

ABSTRACT: Organic light-emitting diodes (OLEDs) have been widely used, particularly in display applications. OLEDs are easily degraded without stringent encapsulation owing to their susceptibility to water vapor and oxygen. Therefore, establishing an effective protection method for these devices is essential. In this study, we demonstrate the device protection performance and improvement in color purity by introducing CaF₂/ZnS multilayered films on a top-emitting inverted-type OLED (iOLED), which was originally intended to act as a distributed Bragg reflector (DBR). To test the protection performance of each dielectric layer, conventional bottom-emitting OLEDs (cOLEDs) with and without single layers of CaF₂ and ZnS were investigated for comparison. All OLEDs were stored in an atmosphere without stringent encapsulation, such as a cover glass. The luminescence area of cOLEDs without the dielectric film decreased by more than 90% after 3 days of fabrication. In contrast, the dark-spot formation was moderated after the same period for the dielectric single-layer deposited cOLEDs. Notably, the iOLED with DBR completely preserved the emitting area even after 2 months of fabrication. This suggests that DBR acted as a protective film for the organic layer, whereas the inverted structure also contributed to reducing the degradation of air- and moisture-sensitive materials.
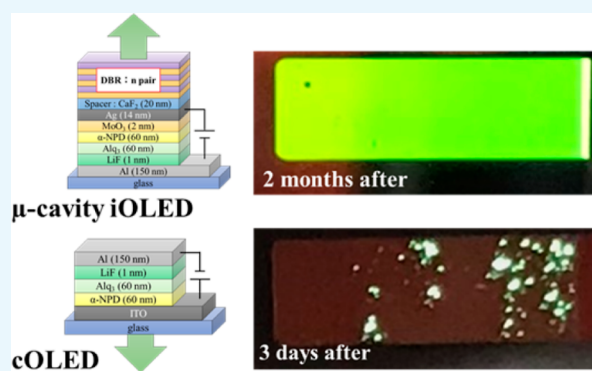
1. INTRODUCTION

In recent years, organic light-emitting diode (OLED) displays have attracted considerable interest because of their advantages, such as fast response time, light weight, low cost, and flexibility.[1−3] In addition to these advantages, OLEDs are expected to emerge as mainstream displays in the future because they can be fabricated on flexible substrates.[4−8] However, OLEDs have the disadvantage of the rapid degradation of the materials and reduction of the light-emitting area. The materials (LiF and Al) used in the device structure for electrodes and the electron injection layer are easily degraded by atmospheric oxygen and water vapor. Consequently, a non-light-emitting area called a dark spot is formed without stringent encapsulation.[9] Therefore, it is necessary to develop high-performance thin-film encapsulation technology to realize an OLED display that can be driven in the atmosphere for a long time. Currently, the most commonly used method is to fabricate an OLED and then rigorously encapsulate it with a cover glass using an ultraviolet (UV)-epoxy resin. The UV-epoxy resin cannot completely prevent the ingress of water vapor in the atmosphere; therefore, a strong desiccant must be sealed with an OLED. Although this method of encapsulation applies to bottom-emission OLEDs,

an opaque desiccant may inhibit emission extraction in top-emission OLEDs. Furthermore, when using a flexible substrate for OLEDs, encapsulation films and desiccants require flexibility. Therefore, it is necessary to develop methods for encapsulating and preventing degradation that can be applied to flexible substrates.[10]

Improvements in the device lifetimes of OLEDs using inorganic materials, polymers, and inorganic/organic hybrid materials have been reported.[10−15] Kim et al. used polyacrylate as a protective layer in a spin-coating method and found that the lifetime of the device reached 12.6 h.[12] Ogawa et al. confirmed that SiN$_X$/SiO$_X$N$_Y$ fabricated via catalytic chemical vapor deposition (Cat-CVD) protects OLEDs at 60 °C and 90% RH for 1000 h,[14] and Ghosh et al. confirmed that an Al₂O₃ layer fabricated using atomic layer deposition (ALD) protects OLEDs at 85 °C and 85% RH for 1300 h.[15] As in
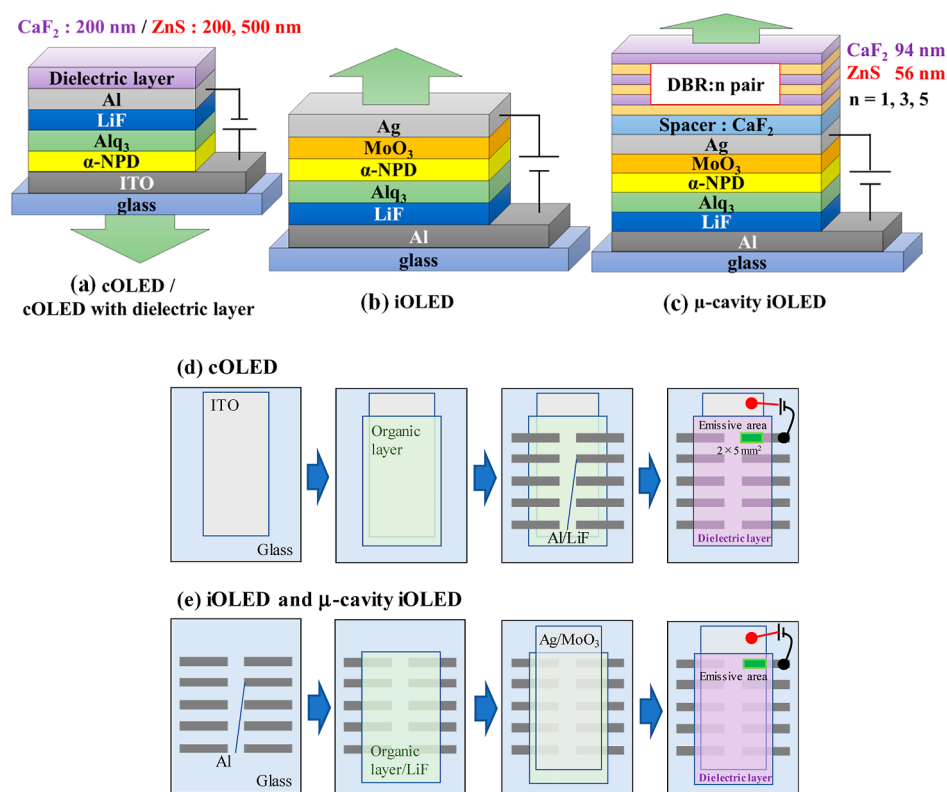
Figure 1. Fabricated device structures of green OLEDs: (a) bottom-emission cOLED with and without a single dielectric layer of CaF_2 and ZnS. (b) Top-emission iOLED. (c) μ-cavity iOLED with different pairs of CaF_2/ZnS DBR. Geometry, size, and order of each deposited layer of (d) cOLED and (e) iOLED and μ-cavity iOLED.

these studies, Cat-CVD and ALD are widely used to produce high-quality protective films.[12−15] However, high-temperature deposition with substrate heating is usually necessary while using these deposition methods, and it may cause damage to the organic layers during the deposition process. In contrast, thermal evaporation can be suitable because it is a relatively gentle deposition method with comparatively low kinetic energy, without introducing plasma in the chamber or corrosive chemical reaction. If these sealing films can be formed using the simple vacuum deposition method, which is facile and is also used to form organic layers, it may be possible to realize long-life device structures with a simpler manufacturing process, considering the affinity toward the existing deposition processes.

Another issue that needs to be considered in OLED display applications is color purity. The triangles formed by the red, blue, and green vertices in the color coordinates indicate the color area that can be represented in a display. The range of colors that can be represented needs to be expanded to display an image closer to what the eye can see. However, improvements are required because the organic light-emitting materials used in conventional OLEDs (cOLEDs) generally have a wide spectral range, and the mixing of various light wavelength components results in low color purity and a narrow range of colors that can be expressed. Currently, two approaches are being explored for improving the color purity: using properly designed light-emitting materials and using resonators. For example, the modification of the molecular design from $Ir(ppy)_3$ to $Ir(mtfppy)_3$, a phosphorescent luminescent material, resulted in a narrower emission spectrum and improved color purity in the green region.[16] In another

method, an optical resonator (cavity) composed of two mirrors was incorporated into the OLED device. By adjusting the cavity length (optical film thickness) between the mirrors, a certain wavelength of light can be selectively extracted, resulting in a narrow electroluminescence (EL) spectrum and improved color purity.[17−22]

In our previous study, the color purity of green OLEDs was improved by introducing a distributed Bragg reflector (DBR) fabricated via vacuum deposition on top of an OLED device with an inverted structure.[23] The previous report focused only on improving the color purity, but herein, we consider that this multilayer film could also work as a protective layer for OLEDs. Selection of the dielectric materials such as calcium fluoride (CaF_2) for low-index and zinc sulfide (ZnS) for high-index is suitable for depositing the multilayered films on the OLED device because they can deposit by the thermal vacuum evaporation method at room temperature with enough optical quality.[24] The room temperature deposition also allows for application to the encapsulation of OLEDs on flexible substrates with low heat tolerance. In this study, we performed three experiments: (1) the deposition of a single layer of a dielectric material (CaF_2 and ZnS) on a cOLED to investigate the protection performance of each layer; (2) the investigation of the impact of using a reversing structure on the dark-spot formation, which makes the layer prone to degradation and less exposed to the atmosphere; and (3) the durability test of the OLED device with both dielectric multilayers (DBR) and a reversed structure. The results showed that the inverted OLED structure with DBR prevented dark-spot formation for more than 2 months after fabrication, even without further encapsulation. This is probably because of the inverted

structure and film formation of the DBR covering the OLED. In terms of color purity, the full width at half maximum (fwhm) of the EL spectrum of the DBR-based OLED could be significantly narrowed from 70 to 19 nm owing to the microcavity effect.

2. MATERIALS AND METHODS

The cOLEDs were fabricated on the commercially available glass substrates coated with an indium tin oxide (ITO) layer that was ultrasonically cleaned with acetone and isopropyl alcohol, followed by UV ozone cleaning. Inverted structure OLEDs (iOLEDs) were fabricated on glass substrates that were ultrasonically cleaned with detergent, purified water, and ethanol, followed by UV ozone cleaning. The detailed sample structures and the geometry, size, and order of each layer of cOLED, iOLED, and μ-cavity iOLED are shown in Figure 1.

All the organic and dielectric films as well as the metal electrodes fabricated in this study were prepared using the thermal vacuum evaporation method at room temperature without substrate heating. The entire process was done in a high vacuum chamber ($<4 \times 10^{-4}$ Pa). During the deposition, the film thickness and deposition rate were controlled by monitoring the quartz crystal microbalance. Ag and Al wires (4 N grade) were employed as the anode and cathode materials, respectively. As the light-emitting layer, tris(8-hydroxyquinolinato)aluminum (Alq_3) was used for the green-emitting OLED. LiF, MoO_3, and N,N'-di-1-naphthyl-N,N'-diphenylbenzidine (α-NPD) were used for the electron injection, hole injection, and hole transport layers, respectively. Calcium fluoride powder (CaF_2, 99.9% purity) and zinc sulfide powder (ZnS, 99.999% purity) were used for the evaporation source of dielectric layers. The film thickness of the DBR fabricated in this study was determined to satisfy Bragg's conditions with the target wavelength of 535 nm for the center of stopband.

The device characteristics were measured using a source measure unit (Keithley 2401) and a chromameter (Konica Minolta, CS-200). A multi-channel spectrometer (Ocean Optics, USB4000) was used for recording the EL spectra. The fabricated OLEDs were stored in a desiccator without being strictly sealed with a cover glass and were not energized to observe the changes over time.

3. RESULTS AND DISCUSSION

3.1. Protection Performance of a Single-Layer Dielectric Film.
First, we examined the protection performance of the single-layer dielectric film against the formation of dark spots in cOLEDs without stringent encapsulation using a cover glass. Single layers of CaF_2 (200 nm) and ZnS (200 and 500 nm) were deposited on cOLED devices. The cOLED device structure was ITO/α-NPD (60 nm)/Alq_3 (60 nm)/LiF (1 nm)/Al (150 nm). Figure 2a shows images of the changes in the emitting area of each OLED device, and the emissive area of each device is plotted against the time of fabrication.

Because the cOLEDs were not stringently encapsulated, the dark spots were spread over the entire area of the device, resulting in a 90% decrease in the emissive area without dielectric coating 3 days after the fabrication. This is probably because of the degradation of Al and LiF located near the top side of the device. In contrast, by depositing a 200 nm CaF_2 or ZnS single layer protection film on top of the cOLED, the dark-spot formation was moderated because the dielectric
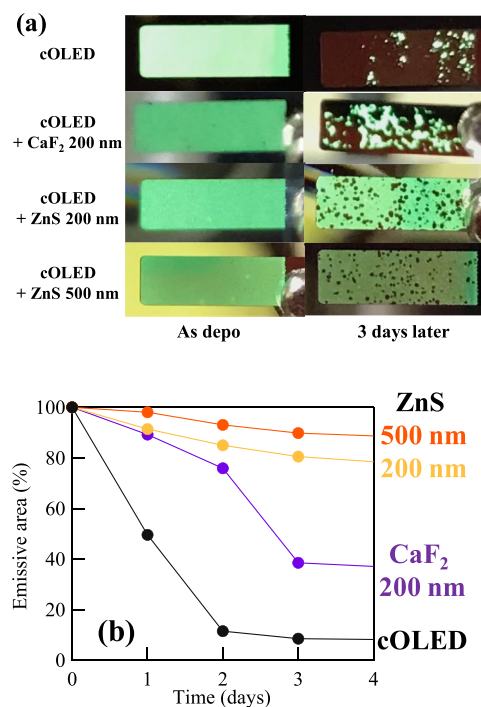

Figure 2. (a) Photographs of the emission pattern of cOLED with and without single-layer dielectric films taken immediately and 3 days after the fabrication. (b) Time-dependent changes in the emissive area as a function of days of cOLED with and without single-layer dielectric films.

material covered the device, which inhibited contact with oxygen and water vapor that caused degradation. There was also a difference in the protection performance between the materials; the emitting area using the CaF_2 film was reduced to 38% after 3 days, whereas it was retained at 80% using ZnS, indicating a better protection performance of ZnS compared to that of CaF_2. This is consistent with a previous report that stated that ZnS is more resistant to heat and the environment.[10] Furthermore, by increasing the film thickness, the ZnS 500 nm device retained 90% of its emissive area even after 3 days of fabrication, indicating that the protective performance was further improved.

As shown in Figure 1, the emissive area is the 2×5 mm^2 section, where both the electrodes overlap each other. When a dielectric protective layer is deposited, at least 2 to 3 mm of the area around the emissive area is surely covered by the dielectric layer. In the case of protection performance with CaF_2, as shown in Figure 2a, the area around the emissive area is noticeably darkened, but at least when ZnS encapsulation is used, the generation of non-emissive areas from the surroundings is significantly suppressed. Therefore, the dielectric film coating prevents the deterioration of the device due to water vapor and oxygen penetration from the side of the films.

3.2. cOLED vs iOLED.
Next, we investigated the effectiveness of adopting an inverted structure to suppress dark-spot formation, where it is more difficult to expose the moisture-sensitive layers (Al and LiF) to the atmosphere, by swapping the positions of the anode and cathode. The effect of the inverted structure on the device performance was reported by Fukagawa et al.[25] They succeeded in suppressing the degradation of OLEDs by employing an inverted structure using the bottom ITO as the cathode. By developing electron

injection materials, a device performance comparable to that of a cOLED with a longer lifetime was achieved for the iOLED even when using the bottom ITO cathode, and no change in the EL spectrum was observed.

In the present study, we did not change the material of the Al cathode but simply swapped the position of the bottom and top surfaces to reduce the degradation of the Al and LiF layers by avoiding exposure to the atmosphere. In addition, we employed a Ag thin-film anode instead of ITO for the top electrode, thereby expecting an improvement in conductivity and color purity owing to the microcavity effect between the reflective electrodes. The device structure consisted of Al (150 nm)/LiF (1 nm)/Alq_3 (60 nm)/α-NPD (60 nm)/MoO_3 (2 nm)/Ag (14 nm). Figure 3 shows the protection performance against the dark-spot formation.
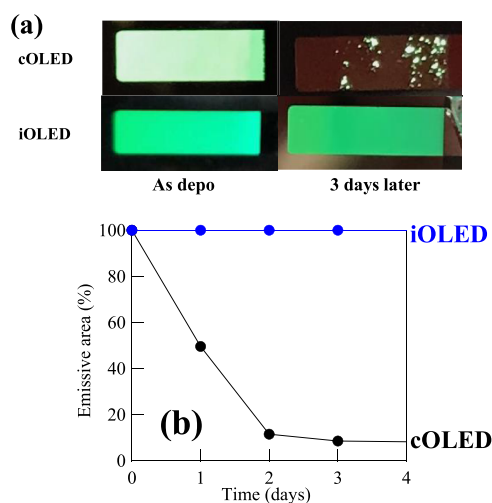

Figure 3. (a) Photographs of the emission pattern of cOLED and iOLED taken immediately and 3 days after the fabrication. (b) Time-dependent changes in the emissive area as a function of days of cOLED and iOLED.

No dark spots were observed for the iOLED even after 3 days of fabrication. This indicates that the Al and LiF layers, which are prone to degradation, have moved to the bottom of the device in the inverted structure, providing more effective protection compared to the dielectric layer coating. The device performance of the iOLED was affected by swapping the positions of the electrodes and employing the Ag anode, as shown in Figure 4a–c and Table 1.

From the current density–voltage–luminance (J–V–L) characteristics shown in Figure 4a,b, the threshold voltage of the iOLED was increased to 4.0 V compared to 2.8 V of the cOLED. This increase probably originated from the difference in the work function of ITO and Ag by inserting the MoO_3 layer, which was already confirmed in the study of green OLED with Ag electrodes,[26] whereas the interface roughness of the electrode can also be a factor affecting the work function because the film position (and the order of deposition) of the anode is different for the cOLED and iOLED. However, the current efficiency of the iOLED is comparable to that of the cOLED, as shown in Figure 4c. This indicated that the recombination process itself was not affected by the introduction of the inverted structure.

3.3. μ-Cavity iOLED. In this section, we describe the fabrication of a μ-cavity iOLED by depositing a dielectric DBR
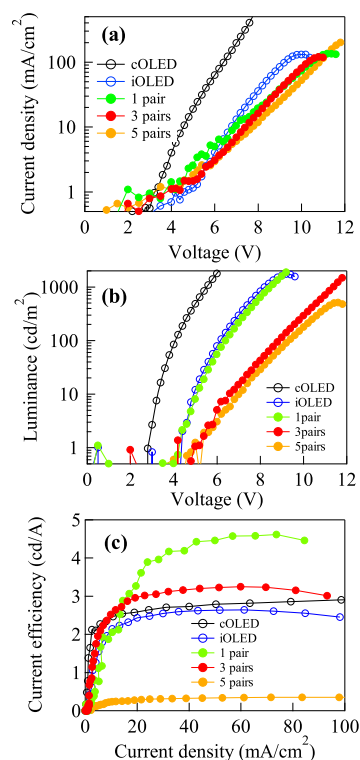

Figure 4. (a) J–V (current density–voltage) and (b) L–V (luminance–voltage) characteristics and (c) current efficiency of cOLED (black open circle), iOLED (blue open circle), and μ-cavity iOLEDs with 1 (green filled circle), 3 (red filled circle), and 5 (yellow filled circle) pairs of DBR.

Table 1. Device Performance of cOLED, iOLED, and μ-Cavity iOLEDs with 1, 3, and 5 Pairs of DBR

	cOLED	iOLED	1 pair	3 pairs	5 pairs
current efficiency at 50 mA/cm² (cd/A)	2.79	2.63	4.46	3.23	0.34
external quantum efficiency at 20 mA/cm²	1.54%	0.83%	1.36%	0.88%	0.08%

on the top surface of iOLED to improve the color purity as well as the protection performance of the device. The thickness of the CaF_2/ZnS DBR was designed for the emission peak at 520 nm, and the number of pairs was prepared as 1, 3, and 5. The thicknesses of the CaF_2/ZnS films were set to 94 nm/56 nm, respectively. Figure 4a–c shows the device characteristics of the fabricated OLEDs. There was a slight increase in threshold voltages among the μ-cavity iOLEDs compared to the cOLED, whose values were close to those of the iOLED without DBR from the J–V curves (Figure 4a). This is reasonable because the deposition position of the DBR is outside the device and may not affect the electrical properties. In the (luminance–voltage) L–V characteristics, the luminance of the three- and five-pair DBR μ-cavity OLEDs showed a slightly lower performance, which probably reflects the spectral narrowing and the matching of the maximum luminosity function and EL peak. When we compared the current efficiency, there was negligible change upon changing the structure from cOLED to iOLED, as mentioned in the previous section, but the OLED device with one or three pairs of DBR outperformed the cOLED. This may be because of the contribution of the microcavity effect induced by the outer
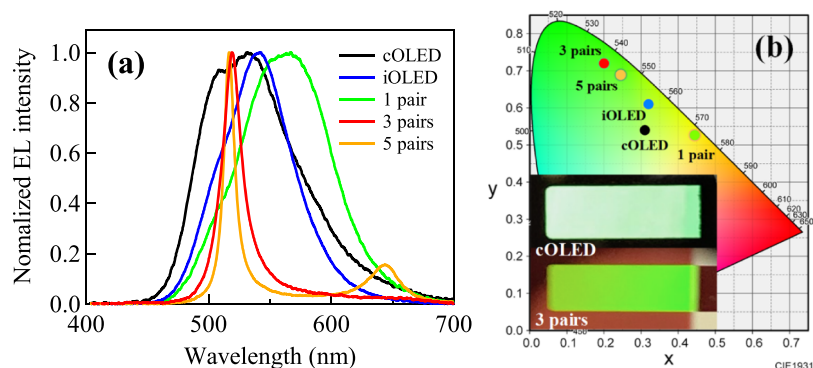
Figure 5. (a) EL spectra of cOLED (black), iOLED (blue), and μ-cavity iOLEDs with 1 (green), 3 (red), and 5 (yellow) pairs of DBR. EL spectra were normalized at the EL peak intensity. (b) Color coordinates in CIE1931 color space of cOLED, iOLED, and μ-cavity iOLEDs with 1, 3, and 5 pairs of DBR, and the inset shows the photographs of the emission pattern of cOLED and μ-cavity iOLEDs with three pairs of DBR.

Table 2. fwhm of the Peaks of EL Spectra and Color Coordinates of CIE for cOLED, iOLED, and μ-Cavity iOLEDs with 1, 3, and 5 Pairs DBR

	cOLED	iOLED	1 pair	3 pairs	5 pairs
fwhm (nm)	93	69	86	19	12
CIE (X, Y)	(0.31, 0.54)	(0.32, 0.61)	(0.44, 0.53)	(0.20, 0.72)	(0.24, 0.69)

DBR mirror and bottom Al electrode. Figure 5 shows the EL spectra and color coordinates.

Three and five pairs of DBR showed significantly narrowed spectra at 520 nm, which is consistent with the designed cavity length and exhibits high wavelength selectivity. The fwhm of the peaks of EL spectra is summarized in Table 2.

The spectral width of the main peak was significantly narrowed to 12 nm for the iOLED with five pairs of DBR compared to 93 nm for the cOLED. The microcavity effect is effective in narrowing the peaks of the EL spectra as the number of DBR pairs increases. The EL spectral peaks of the iOLED without DBR were also narrower than those of the cOLED, which is probably because of the microcavity effect between the Ag and Al electrodes. The one pair case showed an exceptional result of broadened and red-shifted EL spectra, although the current efficiency was better than that of other iOLEDs. Comparing the color purity of the EL spectra in Figure 5b, the μ-cavity iOLED with three pairs of DBR showed the highest color purity for green emission. According to the fwhm data of the EL spectra, the iOLED with five pairs of DBR is expected to possess the best color purity because the peak wavelength is set to 520 nm. However, a sub-peak was observed at 650 nm in the EL spectrum of the iOLED with five pairs of DBR. This was due to the transmission of emission slightly outside the stopband of the DBR because the spectral edge of the stopband becomes steeper with an increase in the number of pairs.

Figure 6 shows the changes in the device characteristics of the three-pair DBR μ-cavity iOLED over time. In the $J-V-L$ characteristics, the current and luminance values gradually decrease with time in the high voltage range, but they are maintained at a certain degree in the low voltage region.

As shown in Figure 6c, the current efficiency was maintained for up to 3 weeks after fabrication, indicating that the degradation of the OLED was suppressed. However, gradual degradation was observed after 2 months. One possible reason for this decrease in the device performance is the degradation of the Ag electrode. Because the Ag electrode for the contact was not protected by the dielectric layer in our device design,
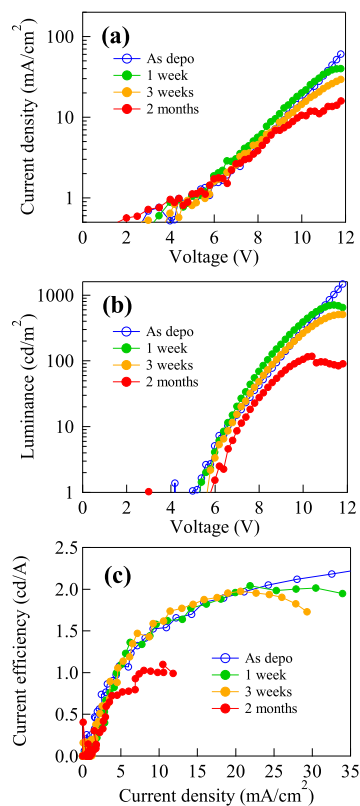

Figure 6. Time-dependent changes in (a) $J-V$ (current density–voltage) and (b) $L-V$ (luminance–voltage) characteristics and (c) current efficiency of μ-cavity iOLEDs with 3 pairs of DBR.

exposure to air caused agglomeration, resulting in a discontinuity in the film. This can increase the resistance of the film, resulting in a decrease in the luminous efficiency.

Figure 7 shows the images of the emitting area of the μ-cavity iOLED with three pairs of DBR, showing that a negligible number of dark spots were formed even 2 months
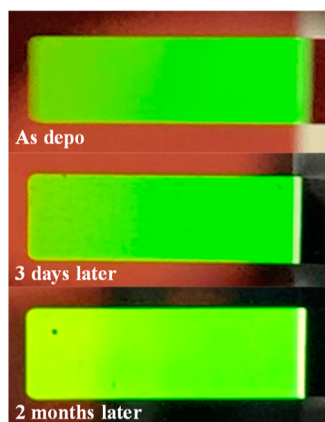
Figure 7. Photographs of the emission pattern of μ-cavity iOLEDs with 3 pairs of DBR taken after deposition and 3 days and 2 months after the device fabrication.

after the fabrication, without stringent encapsulation, such as using a cover glass.

This protection against dark-spot formation was achieved by coating the dielectric multilayer film on top of the device and employing an inverted-type device structure. In this μ-cavity iOLED structure, the CaF_2/ZnS dielectric multilayer film acts as a DBR and a protective layer from the atmosphere. The materials used in this study can be deposited via thermal vacuum evaporation, which is commonly used for fabricating organic layers and metal electrodes in OLEDs. Therefore, it is easier to deposit multifunctional layered films for device protection and improving performance. Further extension of the device lifetime is expected by combining it with the existing encapsulation method.

4. CONCLUSIONS

Different pairs of CaF_2/ZnS multilayered films were deposited on the top-emitting inverted-type OLED, and their optical properties were examined as DBR for improving the color purity. In addition, the role of the protective dielectric coating in inhibiting dark-spot formation in the emissive area was studied. First, we investigated the device protection performance of a single layer of the dielectric material (CaF_2 and ZnS) deposited on a cOLED and confirmed its ability to inhibit dark-spot formation to a certain degree. Second, we investigated the impact of using the inverted structure of the OLED, where the positions of the anode and cathode were swapped, on the dark-spot formation. The iOLED showed a significant inhibition of dark-spot formation by reducing the exposure of the oxygen-sensitive layer to moisture and/or atmosphere. Finally, we fabricated μ-cavity iOLEDs with different pairs of DBR, which possess both confirmed protection characteristics. The results showed that the iOLED with three pairs of DBR prevented dark-spot formation for more than 2 months after fabrication, even without a stringent encapsulation process. In terms of color purity, the full width at half maximum of the peaks of the EL spectrum of the DBR-based OLED could be significantly narrowed from 70 to 19 nm owing to the microcavity effect. Depositing multilayered dielectric films on the top-emitting iOLED using a simple thermal vacuum evaporation method, which is a familiar method for fabricating OLED devices, will be a convenient way to provide the multi-functionality of color purity and device lifetime enhancements.

AUTHOR INFORMATION

Corresponding Author

Takayuki Kiba − Department of Materials Science and Engineering, Kitami Institute of Technology, Kitami 090-8507, Japan; orcid.org/0000-0001-6543-2558; Email: tkiba@mail.kitami-it.ac.jp

Authors

Naoya Satoh − Department of Materials Science and Engineering, Kitami Institute of Technology, Kitami 090-8507, Japan

Tsubasa Tanno − Department of Materials Science and Engineering, Kitami Institute of Technology, Kitami 090-8507, Japan

Takuya Kitabayashi − Department of Materials Science and Engineering, Kitami Institute of Technology, Kitami 090-8507, Japan

Midori Kawamura − Department of Materials Science and Engineering, Kitami Institute of Technology, Kitami 090-8507, Japan

Yoshio Abe − Department of Materials Science and Engineering, Kitami Institute of Technology, Kitami 090-8507, Japan

Complete contact information is available at:
https://pubs.acs.org/10.1021/acsomega.2c01128

Notes

The authors declare no competing financial interest.

REFERENCES

(1) Adachi, C.; Lee, S.; Nakagawa, T.; Shizu, K.; Goushi, K.; Yasuda, T.; Potscavage, W. J., Jr. Organic Light-Emitting Diodes (OLEDs): Materials, Photophysics, and Device Physics. In *Organic Electronics Materials and Devices*; Ogawa, S., Ed.; Springer, 2015; pp 43−73.

(2) Adachi, C. Third-generation organic electroluminescence materials. *Jpn. J. Appl. Phys.* **2014**, 53, 060101.

(3) Mizukami, M.; Cho, S.-I.; Watanabe, K.; Abiko, M.; Suzuri, Y.; Tokito, S.; Kido, J. Flexible organic light-emitting diode displays driven by inkjet-printed high-mobility organic thin-film transistors. *IEEE Electron Device Lett.* **2018**, 39, 39−42.

(4) Park, C. I.; Seong, M.; Kim, M. A.; Kim, D.; Jung, H.; Cho, M.; Lee, S. H.; Lee, H.; Min, S.; Kim, J.; Kim, M.; Park, J.-H.; Kwon, S.; Kim, B.; Kim, S. J.; Park, W.; Yang, J.-Y.; Yoon, S.; Kang, I. World's first large size 77-inch transparent flexible OLED display. *J. Soc. Inf. Disp.* **2018**, 26, 287−295.

(5) Lee, S.-M.; Kwon, J. H.; Kwon, S.; Choi, K. C. A review of flexible OLEDs toward highly durable unusual displays. *IEEE Trans. Electron Devices* **2017**, 64, 1922−1931.

(6) Yokota, T.; Zalar, P.; Kaltenbrunner, M.; Jinno, H.; Matsuhisa, N.; Kitanosako, H.; Tachibana, Y.; Yukita, W.; Koizumi, M.; Someya, T. Ultraflexible organic photonic skin. *Sci. Adv.* **2016**, 2, No. e1501856.

(7) Garner, S.; Chowdhury, D.; Lewis, S. Ultrathin glass substrates for thin, lightweight, flexible OLED lighting. *Inf. Disp.* **2019**, 35, 9−13.

(8) Fukagawa, H.; Sasaki, T.; Tsuzuki, T.; Nakajima, Y.; Takei, T.; Motomura, G.; Hasegawa, M.; Morii, K.; Shimizu, T. Long-lived flexible displays employing efficient and stable inverted organic light-emitting diodes. *Adv. Mater.* **2018**, *30*, 1706768.

(9) Azrain, M. M.; Mansor, M. R.; Fadzullah, S. H. S. M.; Omar, G.; Sivakumar, D.; Lim, L. M.; Nordin, M. N. A. Analysis of mechanisms responsible for the formation of dark spots in organic light emitting diodes (OLEDs): A review. *Synth. Met.* **2018**, *235*, 160−175.

(10) Liao, Y.; Yu, F.; Long, L.; Wei, B.; Lu, L.; Zhang, J. Low-cost and reliable thin film encapsulation for organic light emitting diodes using magnesium fluoride and zinc sulfide. *Thin Solid Films* **2011**, *519*, 2344−2348.

(11) Jeong, Y. S.; Ratier, B.; Moliton, A.; Guyard, L. UV-visible and infrared characterization of poly(p-xylylene) films for wave-guide applications and OLED encapsulation. *Synth. Met.* **2002**, *127*, 189−193.

(12) Kim, G. H.; Oh, J.; Yang, Y. S.; Do, L.-M.; Suh, K. S. Encapsulation of organic light-emitting devices by means of photopolymerized polyacrylate films. *Polymer* **2004**, *45*, 1879−1883.

(13) Charton, C.; Schiller, N.; Fahland, M.; Holländer, A.; Wedel, A.; Noller, K. Development of high barrier films on flexible polymer substrates. *Thin Solid Films* **2006**, *502*, 99−103.

(14) Ogawa, Y.; Ohdaira, K.; Oyaidu, T.; Matsumura, H. Protection of organic light-emitting diodes over 50000 hours by Cat-CVD SiN_x/SiO_xN_y stacked thin films. *Thin Solid Films* **2008**, *516*, 611−614.

(15) Ghosh, A. P.; Gerenser, L. J.; Jarman, C. M.; Fornalik, J. E. Thin-film encapsulation of organic light-emitting devices. *Appl. Phys. Lett.* **2005**, *86*, 223503.

(16) Fukagawa, H.; Oono, T.; Iwasaki, Y.; Hatakeyama, T.; Shimizu, T. High-efficiency UltraPure green organic light-emitting diodes. *Mater. Chem. Front.* **2018**, *2*, 704−709.

(17) Meister, S.; Brückner, R.; Sudzius, M.; Fröb, H.; Leo, K. Optically pumped lasing of an electrically active hybrid OLED-microcavity. *Appl. Phys. Lett.* **2018**, *112*, 113301.

(18) Fukuda, T.; Wei, B.; Ohashi, M.; Ichikawa, M.; Taniguchi, Y. High coupling efficiency of microcavity organic light-emitting diode with optical fiber for as light source for optical interconnects. *Jpn. J. Appl. Phys.* **2007**, *46*, 642−646.

(19) Lin, C.-L.; Lin, H.-W.; Wu, C.-C. Examining microcavity organic light-emitting devices having two metal mirrors. *Appl. Phys. Lett.* **2005**, *87*, 021101.

(20) Dirr, S.; Wiese, S.; Johannes, H.-H.; Kowalsky, W. Organic Electro- and Photoluminescent microcavity devices. *Adv. Mater.* **1998**, *10*, 167−171.

(21) Lim, J.; Oh, S. S.; Kim, D. Y.; Cho, S. H.; Kim, I. T.; Han, S. H.; Takezoe, H.; Choi, E. H.; Cho, G. S.; Seo, Y. H.; Kang, S. O.; Park, B. Enhanced out-coupling factor of microcavity organic light-emitting devices with irregular microlens array. *Opt. Express* **2006**, *14*, 6564−6571.

(22) Schütte, B.; Gothe, H.; Hintschich, S. I.; Sudzius, M.; Fröb, H.; Lyssenko, V. G.; Leo, K. Continuously tunable laser emission from a wedge-shaped organic microcavity. *Appl. Phys. Lett.* **2008**, *92*, 163309.

(23) Kitabayashi, T.; Asashita, T.; Satoh, N.; Kiba, T.; Kawamura, M.; Abe, Y.; Kim, K. H. Fabrication and characterization of microcavity organic light-emitting diode with CaF_2/ZnS distributed Bragg reflector. *Thin Solid Films* **2020**, *699*, 137912.

(24) Muallem, M.; Palatnik, A.; Nessim, G. D.; Tischler, Y. R. Room Temperature Fabrication of Dielectric Bragg Reflectors Composed of a CaF_2/ZnS Multilayered Coating. *ACS Appl. Mater. Interfaces* **2015**, *7*, 474−481.

(25) Fukagawa, H.; Morii, K.; Hasegawa, M.; Arimoto, Y.; Kamada, T.; Shimizu, T.; Yamamoto, T. Highly efficient and air-stable inverted organic light-emitting diode composed of inert materials. *Appl. Phys. Express* **2014**, *7*, 082104.

(26) Kawamura, M.; Ishizuka, Y.; Yoshida, S.; Abe, Y.; Kim, K. H. Ag thin film on an organic silane monolayer applied as anode of organic light emitting diode. *Thin Solid Films* **2013**, *532*, 7−10.